OCTOBER 1980 LRP 174/80

DISPERSION RELATION OF AN ION CYCLOTRON WAVE IN A CYLINDRICAL WAVEGUIDE PARTIALLY FILLED WITH PLASMA IN AN AXIAL MAGNETIC FIELD

P. Kohler and E.S. Weibel

Dispersion Relation of an Ion Cyclotron Wave in a Cylindrical Waveguide partially Filled with Plasma and an Axial Magnetic Field

P. Kohler and E.S. Weibel

Centre de Recherches en Physique des Plasmas

Association Euratom - Confédération Suisse

Ecole Polytechnique Fédérale de Lausanne

CH-1007 Lausanne / Switzerland

ABSTRACT

Continuity of the radial electric displacement and the tangential field components select discrete values for the plasma radius in the partially filled waveguide with static axial magnetic field. The dispersion relation is thus obtained in a parametrised form but the parameter (plasma radius) could be eliminated numerically to yield the usual wavenumber squared versus frequency relation. The plasma radius necessary to satisfy the boundary conditions is found to decrease strongly with respect to the completely filled waveguide as a thin layer of vacuum is added between the wall and the plasma.

Numerical results for the plasma radius dependence on frequency, parallel wavenumber and plasma - wall separation are given for Neon, Xenon and Uranium plasmas.

1. Introduction

An isotope separation method which uses the ponderomotive force produced by a left circularly polarized wave on a plasma has been proposed[1] and numerically studied[2].

The limiting case of a spatially homogeneous plasma is amenable to analytical solution which is presented herein. This corresponds to a sufficiently weak enrichment of the minority ions and very small density modification so that the plasma frequencies are essentially constant throughout the plasma and therefore solves the problem of the fields, surface currents and charges produced by a wave of small amplitude.

Design information for an antenna which excites preferentially this mode is thus obtained in that the resulting surface current distribution should be approximated to produce - by reciprocity - with high efficiency the desired wave.

The behaviour of the plasma radius necessary to satisfy the boundary conditions is analyzed analytically for the more realistic case where the plasma is separated from the conducting wall by a tiny layer of vacuum. It is found to decrease strongly as compared to the completely filled guide. This may be of experimental relevance. Numerically we can deal of course with any vacuum thickness.

Results are given for the dependence of the plasma radius on frequency, parallel wavenumber, composition and plasma - wall separation. The dispersion relation $\omega(n_{\parallel})$ is calculated by elimination of the parameter (plasma radius).

2. Solutions for the fields

We consider a cold cylindrical plasma separated from a concentric conducting guide by a layer of vacuum. The dielectric tensor given by Stix[5] and Maxwell's equations are used to find the electromagnetic fields under the assumption that their general form is

$$f(r)\exp\left[i\omega(n_{\parallel}z - t) + i\nu\varphi\right]$$

Using the approach of Weibel[6] (or the coupled equations method [3,4] which gives equivalent expressions) the solutions are (including the constant $2\pi e^{i\nu\pi/2}$ common factor in the amplitudes and dropping the common $\exp\left[i\omega(n_{\parallel}z - t) + i\nu\varphi\right]$ dependence)

a) in the plasma (solutions must be regular at the origin $r = 0$)

$$E_r = \sum_{\alpha=1,2} A_\alpha \left(-i J_\nu'(\rho^{(\alpha)}) - i\,\varepsilon_{2\alpha}\,\frac{\nu}{\rho^{(\alpha)}} J_\nu(\rho^{(\alpha)})\right) \qquad (1a)$$

$$E_\varphi = \sum_{\alpha=1,2} A_\alpha \left(\frac{\nu}{\rho^{(\alpha)}} J_\nu(\rho^{(\alpha)}) + \varepsilon_{2\alpha}\, J_\nu'(\rho^{(\alpha)})\right) \qquad (1b)$$

$$E_z = \sum_{\alpha=1,2} A_\alpha \varepsilon_{3\alpha} J_\nu(\rho^{(\alpha)}) \tag{1c}$$

$$B_r = \sum_{\alpha=1,2} A_\alpha \left(\beta_{1\alpha} J'_\nu(\rho^{(\alpha)}) - \beta_{2\alpha} \frac{\nu}{\rho^{(\alpha)}} J_\nu(\rho^{(\alpha)}) \right) \tag{1d}$$

$$B_\varphi = \sum_{\alpha=1,2} A_\alpha \left(i\beta_{1\alpha} \frac{\nu}{\rho^{(\alpha)}} J_\nu(\rho^{(\alpha)}) - i\beta_{2\alpha} J'_\nu(\rho^{(\alpha)}) \right) \tag{1e}$$

$$B_z = \sum_{\alpha=1,2} A_\alpha \, i\beta_{3\alpha} J_\nu(\rho^{(\alpha)}) \tag{1f}$$

where the prime means derivation with respect to the argument

$\rho^{(\alpha)} \stackrel{\text{Def}}{=} \frac{\omega}{c} n_\perp^{(\alpha)} r$ which may be imaginary.

b) in the vacuum

$$n^2 = S = R = L = P = 1 \quad \text{and} \quad D = 0$$

Thus ε_z is indeterminate and there are two independent amplitudes A and B corresponding to the transverse electric components whereas the axial component is given by

$$E_z = - \frac{n_\perp}{n_\parallel} A$$

The radial dependence need not be regular at the origin occupied by the plasma and may thus contain linear combinations of Bessel and Neumann functions. The boundary conditions at the vacuum - metal interface may be included directly by normalizing the solutions in such a way as to ensure vanishing of the tangential components of the electric field at the boundary.

The condition on the radial B - component is automatically fulfilled as the solutions satisfy Maxwell's equations.

In the vacuum it is naturally possible to split the solutions into a TM and a TE mode.

They are (with $\rho = \frac{\omega}{c} n_\perp^{(vac)} r$ and $\beta = \frac{\omega}{c} n_\perp^{(vac)} b$ where b is the conducting shell radius)

$$E_r = -A Z_\nu'(\rho) - B \tilde{Z}_\nu(\rho)\, i \frac{\nu}{\rho} \tag{2a}$$

$$E_\varphi = -A\, i \frac{\nu}{\rho} Z_\nu(\rho) + B \tilde{Z}_\nu'(\rho) \tag{2b}$$

$$E_z = A\, i \frac{n_\perp}{n_\parallel} Z_\nu(\rho) \tag{2c}$$

$$B_r = A\, i \frac{\nu}{n_\parallel \rho} Z_\nu(\rho) - B n_\parallel \tilde{Z}_\nu'(\rho) \tag{2d}$$

$$B_\varphi = -A \frac{1}{n_\parallel} Z_\nu'(\rho) - iB n_\parallel \frac{\nu}{\rho} \tilde{Z}_\nu(\rho) \tag{2e}$$

$$B_z = iB n_\perp \tilde{Z}_\nu(\rho) \tag{2f}$$

with

$$Z_\nu(\rho) = \frac{J_\nu(\rho)}{J_\nu(\beta)} - \frac{y_\nu(\rho)}{y_\nu(\beta)} \tag{3a}$$

$$\tilde{Z}_\nu(\rho) = \frac{J_\nu(\rho)}{J_\nu'(\beta)} - \frac{y_\nu(\rho)}{y_\nu'(\beta)} \tag{3b}$$

Generally the arguments ρ and β of the Bessel and Neumann functions J and y are purely imaginary because propagating $(n_\parallel \in \mathbb{R})$ waves with $n_\parallel \gg 1$ are most interesting. Thus $n_\perp^{(vac)} \in \mathbb{I}m$ because

$$n_\perp^{2\,(vac)} + n_\parallel^2 = n^2 - 1$$

3. Implicit dispersion relation

The Z functions obviously ensure $E_z = E_\varphi = 0$ at $\rho = \beta$ as required. The vacuum - metal interface boundary conditions are thus already included in the solutions and we need only the plasma - vacuum interface conditions to close the set of equations. We require the tangential components of the fields to be continuous since we are not interested in surface currents and charges at the plasma boundary. This yields four linear homogeneous equations for the amplitudes A_α $(\alpha = 1,2)$, and A, B which allow to find them up to a multiplicative constant representing the induced field strength at a given point.

The determinant of the coefficients of these equations must vanish for a nontrivial solution of the amplitudes. This produces a transcendental equation for the plasma radius which must be solved numerically in general. It may be written as an equation containing only real terms for cases of interest, but we do not undertake here to do so because this requires distinction between real and imaginary indices $(n_\parallel, n_\perp^{(vac)}, n_\perp^{(A)}, n_\perp^{(B)} \Rightarrow 16$ cases$)$.

The equation is (eq. 5)

$$\begin{vmatrix} -i\frac{\nu}{\zeta}\mathcal{Z}_\nu(\rho) & \widehat{\mathcal{Z}}_\nu'(\rho) & -\frac{\nu}{\zeta^{(1)}}\mathcal{Z}_\nu(\rho^{(1)}) - \varepsilon_{21}\mathcal{J}_\nu'(\rho^{(1)}) & -\frac{\nu}{\zeta^{(2)}}\mathcal{J}_\nu(\rho^{(2)}) - \varepsilon_{22}\mathcal{J}_\nu'(\rho^{(2)}) \\ i\frac{n_\perp^{(ext)}}{n_\parallel}\mathcal{Z}_\nu(\rho) & 0. & -\varepsilon_{31}\mathcal{J}_\nu(\rho^{(1)}) & -\varepsilon_{32}\mathcal{J}_\nu(\rho^{(2)}) \\ -\frac{1}{n_\parallel}\mathcal{Z}_\nu'(\rho) & -in_\parallel\frac{\nu}{\zeta}\widehat{\mathcal{Z}}_\nu(\rho) & -i\beta_{11}\frac{\nu}{\rho^{(1)}}\mathcal{J}_\nu(\rho^{(1)}) + i\beta_{12}\mathcal{J}_\nu'(\rho^{(1)}) & -i\beta_{12}\frac{\nu}{\rho^{(2)}}\mathcal{J}_\nu(\rho^{(2)}) + i\beta_{22}\mathcal{J}_\nu'(\rho^{(2)}) \\ 0. & in_\perp^{(ext)}\widehat{\mathcal{Z}}_\nu(\rho) & -i\beta_{21}\mathcal{J}_\nu(\rho^{(1)}) & -i\beta_{32}\mathcal{J}_\nu(\rho^{(2)}) \end{vmatrix} = 0.$$

For any given $n_\parallel$ and ω inside some domain of definition we may thus find a set of discrete values of the plasma radius which satisfies the boundary conditions. We have thus a parametric representation of the dispersion relation. Numeric techniques are necessary for the elimination of the parameter because of the complicated transcendental nature of the relations and because of the range of the arguments which do not allow expansion for the general case of interest.

4. Approximate analytical results for small or vanishing vacuum thickness

a) Dominant component of the index

Let $n_{\parallel}^2 \approx L$. One of the solutions of the biquadratic equation for the $n_{\perp}$ would then nearly vanish whereas the other is approximately

$$n_{\perp}^{(1)\,2} = \frac{PS + RL - (P+S)L}{S}$$

$$= \frac{\alpha}{\mu}\left(\frac{1}{\mu} + \frac{1}{\varepsilon} - 2\right)$$

with $\alpha = \frac{\omega_{pe}^2}{\omega_{ce}^2}$; $\mu = \frac{m_e}{m_i}$

and ε defined by $\omega = (1+\varepsilon)\,\omega_{ci}$.

The ordering $\frac{1}{\mu} \gg \frac{1}{\varepsilon} \gg 2$ holds for cases of interest which makes $n_{\perp}^{(1)2} \approx \frac{\alpha}{\mu\varepsilon}$ dominate the total index in general. This can be written explicitely in MKS

$$n_{\perp}^{(1)} \approx \frac{c\, m_i}{B}\sqrt{\frac{n_e \mu_0}{m_e}} \qquad (6)$$

b) Approximative plasma radius for the completely filled guide

For the case of vanishing vacuum thickness the equation for a is reduced to the 2 x 2 determinant of the plasma coefficients of E_φ and E_z which

must both vanish at $r = a$.

Since we have seen above that one of the two perpendicular indices dominates by far the other and since the corresponding $|\varepsilon_{21}| \ll 1$ $\left(\varepsilon_{21} = \frac{D}{n^2 - S} \approx \frac{-L/2}{L + n_1^{(1)2} - L/2}\right)$, we must make the argument of the Bessel function nearly equal to a root

$$p_{\nu,m}^{(1)} = \frac{\omega a n_1^{(1)}}{c} \approx j_{\nu,i}$$

For $\nu = \pm 1$ we have $j_{\pm 1,1} = 3.83171\ldots$, and thus

$$a \approx \frac{3.83}{e} \sqrt{\frac{m_e}{\mu_0 n_e}} \qquad (7)$$

making the electron density the parameter which allows to adjust the desired radius.

c) <u>Behaviour of the plasma radius when a tiny layer of vacuum is added between the plasma and the guide</u>

Write the system of boundary conditions at the plasma - vacuum interface as

$$\begin{aligned}
A\,Q_{11} - B\,Q_{12} + C\,Q_{13} + D\,Q_{14} &= 0 \\
A\,Q_{21} \qquad\quad + C\,Q_{23} + D\,Q_{24} &= 0 \\
A\,Q_{31} + B\,Q_{32} + C\,Q_{33} + D\,Q_{34} &= 0 \\
\qquad\quad B\,Q_{42} + C\,Q_{43} + D\,Q_{44} &= 0
\end{aligned}$$

We compute the zero and first order terms of the determinant in the small parameter $\frac{b-a}{a}$ as

$$
\begin{aligned}
\mathrm{Det} \approx\ & Q_{13}Q_{24} - Q_{14}Q_{23} \\
& + Q_{13}\frac{Q_{21}Q_{44}Q_{32}}{Q_{42}Q_{31}} - Q_{13}\frac{Q_{21}Q_{34}}{Q_{31}} \\
& - Q_{24}\frac{Q_{43}Q_{12}}{Q_{42}} + Q_{24}\frac{Q_{11}Q_{43}Q_{32}}{Q_{42}Q_{31}} - Q_{24}\frac{Q_{11}Q_{23}}{Q_{31}} \\
& - Q_{14}\frac{Q_{21}Q_{43}Q_{32}}{Q_{42}Q_{31}} + Q_{14}\frac{Q_{21}Q_{33}}{Q_{31}} \\
& + Q_{23}\frac{Q_{44}Q_{12}}{Q_{42}} - Q_{23}\frac{Q_{11}Q_{44}Q_{32}}{Q_{42}Q_{31}} + Q_{23}\frac{Q_{11}Q_{34}}{Q_{31}} \\
& + O\left(\left(\frac{b-a}{a}\right)^2\right)
\end{aligned}
\tag{8}
$$

The Z functions are expanded (case $\eta_{\parallel} \in \mathbb{R}$ and $\eta_{\perp}^{(vac)} \in \mathrm{Im}$)

$$Z(\rho) \approx \frac{\rho}{\beta} - \frac{\beta}{\rho} \rightarrow \frac{2}{|\rho|}(|\rho| - |\beta|)$$

$$Z'(\rho) \approx \frac{1}{\beta} + \frac{\beta}{\rho^2} \rightarrow \frac{1}{i}\frac{2}{|\rho|}$$

$$\tilde{Z}(\rho) \approx \rho + \frac{\beta^2}{\rho} \rightarrow 2|\rho| i$$

$$\tilde{Z}'(\rho) \approx 1 - \left(\frac{\beta}{\rho}\right)^2 \rightarrow \frac{2}{|\rho|}(|\rho| - |\beta|)$$

and the Bessel functions of the plasma terms

$$\rho^{(1)} = j_{1,1} + \tilde{\varepsilon} \quad : J_1(\rho^{(1)}) \sim \frac{\rho^{(1)} - j_{1,1}}{2} \; ; \; J_1'(\rho^{(1)}) \sim .403 \; ; \; \frac{J(\rho^{(1)})}{\rho^{(1)}} \approx \frac{\rho^{(1)} - j_{1,1}}{2 j_{1,1}}$$

$$\rho^{(2)} \ll 1 \quad : J_1(\rho^{(2)}) \sim \frac{\rho^{(2)}}{2} \; ; \; J_1'(\rho^{(2)}) \sim \frac{J_1(\rho^{(2)})}{\rho^{(2)}} \approx .5$$

Then we use

$$\varepsilon_{2i} = \frac{D}{n_{\parallel}^2 + n_{\perp}^{(i)2} - S} = \frac{-L/2}{L + n_{\perp}^{(i)2} - L/2} \quad \begin{cases} \varepsilon_{11} \ll 1 & \text{for } i = 1 \\ \varepsilon_{22} \sim -1 & \text{for } i = 2 \end{cases}$$

$$\varepsilon_{3i} = \frac{n_{\parallel} n_{\perp}^{(i)}}{n_{\perp}^{(i)2} - P} \approx \frac{n_{\perp}^{(i)} \sqrt{L}}{n_{\perp}^{(i)2} - P} \quad \begin{cases} \gg 1 & \text{for } i = 1 \\ \ll 1 & \text{for } i = 2 \end{cases}$$

and examine every term of eq. (8).

Only the four underscored terms prove to be relevant and yield the equation (to first order in $\frac{b-a}{a}$)

$$\frac{-2 n_{\perp}^{(1)}}{n_{\parallel}(n_{\perp}^{(1)2} - P)} (j_{1,1} - \rho^{(1)}) = (|\varepsilon| - |\beta|) \left(\frac{2(j_{1,1} - \rho^{(1)})}{\rho^{(1)}} + \frac{\nu n_{\parallel} (j_{1,1} - \rho^{(1)})}{|\varepsilon| \, n_{\perp}^{(1)}} \right.$$

$$\left. - 1.6 \frac{P}{n_{\perp}^{(1)2} - P} + 2\nu n_{\parallel} \frac{j_{1,1} - \rho^{(1)}}{|\varepsilon|} \frac{n_{\perp}^{(1)}}{n_{\perp}^{(1)2} - P} \right)$$

Using representative plasma parameters that might be achieved in a real experiment this equation relating the required plasma radius to the plasma parameters and the vacuum thickness may still be simplified, although it can of course be solved as it stands. The underscored term dominates the right hand side of the equation and we obtain

$$a = -.8 \frac{(a-b)\ P\ n_{\parallel}^2}{n_{\perp}^{(1)2}} + \frac{j_{\parallel 1}\ L}{n_{\perp}^{(1)}\ \omega} \qquad (9a)$$

(which confirms the result of 4b) for $(a-b) = 0$) and the derivative

$$\frac{d(a)}{d(b-a)} = .8 \frac{P\ n_{\parallel}^2}{n_{\perp}^{(1)2}} \qquad (9b)$$

which is negative and much bigger than unity (order: 10^4). This establishes the very strong decrease of the required plasma radius as a tiny vacuum layer is added between the guide and the plasma.

The argument can also run as follows :

Of the 14 non-zero terms in the continuity matrix there are six which are not linear in $\rho - \beta$ nor $\xi^{(2)}$ neither $j_{\parallel 1} - \xi^{(1)}$, which are the variables which may become very small. Two of them Q_{14} and Q_{42} are alone in their equation, while the remaining four are all in equation (3) (for B_φ). Thus the most important terms are the four which multiply the two single

terms in the determinant. These are Q_{21}, Q_{23}, Q_{31}, and Q_{33}.

$$Q_{33}\, Q_{21} \quad = \quad Q_{31}\, Q_{23}$$

$$(B\varphi_{pe1})(E_{zvc}) \quad (B\varphi_{vc1})(E_{zpe1})$$

is thus nearly equivalent to Det = 0 and yields (for $\nu = -1$, $n_{\parallel}, n_{\perp}^{(1)} \in \mathbb{R}$, $n_{\perp}^{(vac)} \in \mathrm{Im}$)

$$\left(-i\beta_{21}\, J_{-1}'(\rho^{(1)})\right)\left(-\frac{n_{\perp}}{n_{\parallel}} Z_{-1}(\rho)\right) = \left(-i\frac{1}{n_{\parallel}} Z_{-1}'(\rho)\right)\left(\varepsilon_{31}\, J_{-1}(\rho^{(1)})\right)$$

which is with

$$J_{-1}'(\rho^{(1)})\Big|_{\rho^{(1)} \approx j_{1,1}} \approx .403\ldots$$

$$Z_{-1}(\rho)\Big|_{\rho \approx \beta} \approx \frac{2}{|\beta|}\,(|\beta| - |\beta|)$$

$$Z_{-1}'(\rho)\Big|_{\rho \approx \beta} \approx \frac{1}{i}\,\frac{2}{|\beta|}$$

$$J_{-1}(\rho^{(1)})\Big|_{\rho^{(1)} \approx j_{1,1}} \approx -.403..\,(j_{1,1} - \rho^{(1)})$$

$$\rightarrow \qquad a \approx \frac{c\, j_{1,1}}{n_{\perp}^{(1)}\,\omega} + \frac{n_{\parallel}^2\, p}{n_{\perp}^{(1)2}}\,(b - a) \qquad (10)$$

For higher zeroes of the determinant just replace $j_{\lambda,1}$ by $j_{\lambda,i}$ because both $J_{-i}(\rho^{(\lambda)})$ and $J'_{-i}(\rho^{(\lambda)})$ change sign and the coefficient changes in both expansions at the same rate. This is also true for $\nu = +i$ because both J_{+i} and J'_{+i} change sign with respect to J_{-i} and J'_{-i} whereas the z_ν are unaffected.

5. Numerical Results

The basic hypothesis being that the densities are unperturbed, we always run with the natural isotope concentrations considering only stable and longlived species ($T_{1/2} > 1_{year}$).

These concentrations are [7].

Neon	mass (UMA)	19.99877		20.9996	21.99844	
	conc. (%)	90.51		0.28	9.21	
Xenon	mass (UMA)	124	126	128	129	130	131
	conc. (%)	0.094	0.088	1.90	26.23	4.07	21.17
	mass (UMA)	132	134	136		
	conc. (%)	26.96	10.54	8.95		
Uranium	mass (UMA)	234	235	238		
	conc. (%)	0.00518	0.719	99.274		

The static magnetic field is chosen such as to make a large number of ion Larmor radii fit into the resulting plasma radius which is generally taken as the smallest nontrivial solution. An exception is made when it drops below 0.01 meter.

This leads us to choose .3 Tesla for Neon, 1 Tesla for Xenon and 2.5 Tesla for Uranium.

The densities have a primordial influence on the resulting radii (cf. the section on approximate analytical results). We choose them in such a way as to obtain experimentally realizable conditions, i.e. to obtain radii in the .1 meter range. This leads to electron densities of $4 \cdot 10^{16} m^{-3}$ for Neon and $10^{17} m^{-3}$ for the heavier elements.

Previous results[1,2] indicate that we shall need electric fields of several 100 V/m. We scale thus all fields, charges and currents to

$$|E(r=0, z=0, \varphi=0, t=0)| = 100\ V/m$$

The required antenna currents (I) for some specific cases are displayed in the following table together with the resulting plasma radii (a) and length (L) for a one wavelength machine left wave and .01 m vacuum thickness.

$\underline{\text{Neon}}_{20,22}$; frequency = 219 456 Hz ($\hat{=} \omega_{ci}$ of mass 21)

	I	I_z	a	L
$n_{//}^2 = .95 \times L$	- .49 A/m	- 10.5 A/m	.054 m	8.30 m
$n_{//}^2 = 1.05 \times L$	+ .46 A/m	+ 9.82 A/m	.051 m	7.90 m
$n_{//}^2 = 2.0 \times L$			.035 m	5.70 m

$\underline{\text{Uranium}}_{238,235,234}$; frequency = 162 388 Hz

	I	I_z	a	L*
$n_{//}^2 = .95 \times L$	- .38 A/m	- 2.76 A/m	.125 m	5.69 m
$n_{//}^2 = 1.05 \times L$	+ .37 A/m	+ 2.75 A/m	.117 m	5.41 m

*here $n_{//}^2 < 0$ so that we cannot speak of one wavelength but rather of the e-folding length.

6. Antenna design

Since the fields mus eventually vanish in a sufficiently thick conducting layer the normal component of the electric displacement at $r = b$ (the conducting shell radius) is in MKS equal to the surface charge density and the tangential components of the magnetic field allow us to find the surface current density (equality in MKS of the mutually perpendicular components) which is consistent with the fields in the cavity.

It is thus expected that we might obtain the same fields when exciting corresponding currents and preferentially generate this mode when approaching them sufficiently.

It may be important to generate efficiently the desired mode because electric breakdown occurs if the electric field strength rises too much. This is however inevitable if only a small fraction of the field corresponds to the desired mode because the necessary amplitude of the latter is an experimental constraint related to the limiting separation efficiency.

The $\exp[i(kz-\omega t+\nu\varphi)]$ dependence ($\nu=-1$ for a left wave) imposes already a sinusoidal variation of the current along z and φ which must turn at the angular frequency ω about the cylinder axis and travel along it with a speed of ω/k . The only freedom which is left open is the ratio of the axial to azimuthal currents. This ratio is found numerically to vary with the experimental parameters, but in

general the axial current must be about ten times stronger than the azimuthal current.

A network which would allow to approach this current distribution with arbitrary pitch is a grid of independently dephasable axial and azimuthal segments. The return currents might be shielded by a conducting cylinder of some millimeter wall thickness since the skin depth δ for a $1/e$ attenuation is related to the frequency and material conductivity by

$$\delta = \sqrt{2/\omega\mu_0\sigma}$$

which is about 1.5 mm for copper and 200 KHz ($\sigma = 5.75 \cdot 10^5$ S/m).

Connecting suitably the segments a very large amount of dephasing circuitry can be spared. This is feasible if corresponding numbers of elements are chosen along z and φ and does not limit experimentally because the value of $n_{\parallel}$ (or k) and ν are anyway given from the machine size and the type of wave.

The field induced by this antenna structure can be described in terms of straight segment fields and incomplete elliptic integrals. A numerical code has been written which evaluates it in the absence of plasma. It shows that a considerable number of segments is necessary to approximate the ideal current distribution. This is of course a consequence of the geometry which forces us to work in the near field of the antenna.

Figure Captions

Table 1 : Frequency dependence of plasma radius

for $U_{238, 235, 234}$ $B = 2.5T$ $b-a = .01m$ $n_e = 10^{17}m^{-3}$ $n_{//}^2 = 1.02 \cdot L$ $\nu = -1$

Ordinate : radius is meters
Abscissa : frequency in cycles per second

arrows = cyclotron frequencies of the three isotopes

Inset dispersion relation near the U_{235} resonance and cutoff

Table 2 : Frequency dependence of plasma radius

for $Xe_{124, 126, 128, 129, 130, 131, 132, 134, 136}$

$B = 1.T$ $b - a = 0.01m$
$n_e = 10^{17}m^{-3}$ $n_{//}^2 = 1.02 \cdot L$
$\nu = -1$

Ordinate : radius in meters
Abscissa : frequency in cycles per second

arrows = cyclotron frequencies of the isotopes (length: proporional to their abundance)

Table 3 : Frequency dependence of plasma radius

for $Ne_{20, 22}$ $b-a = 0.01$

$B = .3T$
$n_e = 4 \cdot 10^{16}m^{-3}$ $n_{//}^2 = .95 \cdot 2$
$\nu = -1$

Ordinate : radius in meters
Abscissa : frequency in cycles per second

(The ion cyclotron frequencies of Ne_{20} and Ne_{22} lie immediately below and above the end points of this frequency interval. The Ne_{22} isotope has not been included.)

Table 4 : Plasma radius dependence on length for one full wavelength along the axial direction

for $Ne_{20,22}$

$B = .3T$ $\quad b-a = .01m$
$n_e = 4 \cdot 10^{16} m^{-3}$ $\quad f = 219456$ Hz
$\nu = -1$

Ordinate : plasma radius in meters
Abscissa : parallel index squared ($n_{//}^2$)

L(m) gives the corresponding one wavelength machine length.

Table 5 : Dispersion relation $f(n_{//}^2)$ for $Ne_{20,22}$ above the negative k^2 values near the Ne_{22} resonance and below the Ne_{20} ion cyclotron frequency.

$B = .3T$ $\quad b-a = .01m$
$n_e = 4 \cdot 10^{16} m^{-3}$ $\quad f = 219456$ Hz
$\nu = -1$ $\quad$ Plasma radius = .051m

Abscissa : frequency in Hz
Ordinate : parallel index squared

L(m) gives the corresponding one wavelength machine length.

The last point (50) is at 99.5% of $f_{ciNe_{20}}$ and the first (0) at 101.15% of $f_{ciNe_{22}}$. All these points are thus reasonably accessible since the magnetic field ripple may be kept within less than 1% easily.

Table 6 : Plasma radius dependence on the vacuum layer thickness showing the sharp decrease near zero vacuum width.

$Ne_{20,22}$

$B = .3T$
$n_e = 4 \cdot 10^{16} m^{-3}$ $\quad n_{\phi}^2 = 1.02 \cdot L$
$f = 219\,456$ Hz

Abscissa : vacuum width in meters
Ordinate : plasma radius in meters

Table 7 : Plasma radius dependence on vacuum thickness showing the initially strong decrease and the later increase and levelling leaving still a net gain in radius.

$Ne_{20,22}$

$B = .3T$
$n_e = 4 \cdot 10^{16} m^{-3}$ $\quad n_{\phi}^2 = 1.05 \cdot L$
$f = 219\,456$ Hz

Abscissa : vacuum width in meters
Ordinate : plasma radius in meters

References

1) E.S. Weibel, Separation of Isotopes, Phys.Rev.Lett. 44, 377 (1980)

2) M.C. Festeau-Barrioz, and E.S. Weibel, Report LRP 164/80 CRPP, Ecole Polytechnique Fédérale de Lausanne, February 1980

3) R.A. Gore, and H. Lashinsky, Phys.Fluids 22, 2178 (1979)

4) H. Suhl, and L.R. Walker, Bell System Tech. Journal, p. 579 May 1954 (Vol. 33, Nos. 3,4, and 5)

5) T.H. Stix, The Theory of Plasma Waves, McGraw Hill, 1962 (p. 11 and 20)

6) E.S. Weibel, private communication

7) S.H. Tideström, Manuel de l'Ingénieur, Dunod, 1961

TABLE AND PLOT OF THE FUNCTION AVSF

ABSCISSA PARAMETERS=
LOWER LIMIT... .16069E+06
UPPER LIMIT... .16483E+06
STEP SIZE..... 82.759
POINT NUMBER.. 51

ORDINATE PARAMETERS=
LOWER LIMIT... .87421E-01
UPPER LIMIT... .89762E-01
BIN SIZE..... .23401E-04
BIN NUMBER.... 100

POINT	ABSCISSA	ORDINATE
0	.1607E+06	.88455E-01
1	.1608E+06	.88438E-01
2	.1609E+06	.88423E-01
3	.1609E+06	.88410E-01
4	.1610E+06	.88400E-01
5	.1611E+06	.88397E-01
6	.1612E+06	.88411E-01
7	.1613E+06	.88484E-01
8	.1614E+06	.89762E-01
9	.1614E+06	.87966E-01
10	.1615E+06	.88094E-01
11	.1616E+06	.88118E-01
12	.1617E+06	.88119E-01
13	.1618E+06	.88111E-01
14	.1618E+06	.88098E-01
15	.1619E+06	.88084E-01
16	.1620E+06	.88068E-01
17	.1621E+06	.88050E-01
18	.1622E+06	.88032E-01
19	.1623E+06	.88014E-01
20	.1623E+06	.87995E-01
21	.1624E+06	.87976E-01
22	.1625E+06	.87956E-01
23	.1626E+06	.87936E-01
24	.1627E+06	.87916E-01
25	.1628E+06	.87896E-01
26	.1628E+06	.87875E-01
27	.1629E+06	.87853E-01
28	.1630E+06	.87830E-01
29	.1631E+06	.87806E-01
30	.1632E+06	.87779E-01
31	.1633E+06	.87743E-01
32	.1633E+06	.87659E-01
33	.1634E+06	.88477E-01
34	.1635E+06	.87808E-01
35	.1636E+06	.87752E-01
36	.1637E+06	.87719E-01
37	.1638E+06	.87693E-01
38	.1638E+06	.87669E-01
39	.1639E+06	.87646E-01
40	.1640E+06	.87624E-01
41	.1641E+06	.87602E-01
42	.1642E+06	.87585E-01
43	.1642E+06	.87563E-01
44	.1643E+06	.87542E-01
45	.1644E+06	.87522E-01
46	.1645E+06	.87502E-01
47	.1646E+06	.87482E-01
48	.1647E+06	.87461E-01
49	.1647E+06	.87441E-01
50	.1648E+06	.87421E-01

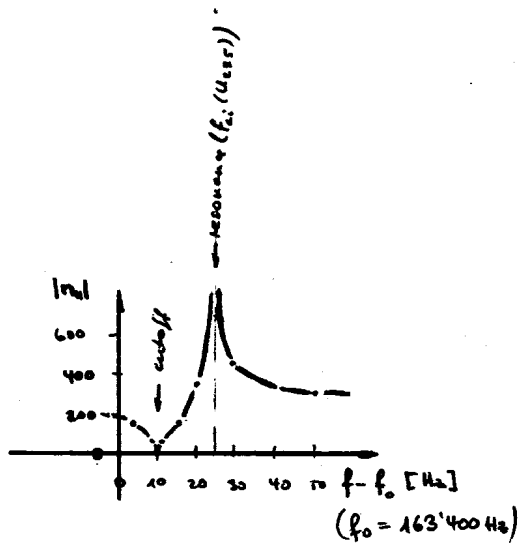

Table 1

ESTIMATE OF INTEGRAL... 364.0

..... TABLE AND PLOT OF THE FUNCTION AVSF .....

ABSCISSA PARAMETERS=
LOWER LIMIT... .11254E+06
UPPER LIMIT... .12439E+06
STEP SIZE..... 236.93
POINT NUMBER.. 51

ORDINATE PARAMETERS=
LOWER LIMIT... .77585E-01
UPPER LIMIT... .90915E-01
BIN SIZE..... .13330E-03
BIN NUMBER.... 100

POINT	ABSCISSA	ORDINATE
0	.1125E+06	.89072E-01
1	.1128E+06	.88744E-01
2	.1130E+06	.87950E-01
3	.1133E+06	.77585E-01
4	.1135E+06	.90915E-01
5	.1137E+06	.89828E-01
6	.1140E+06	.89393E-01
7	.1142E+06	.89075E-01
8	.1144E+06	.88739E-01
9	.1147E+06	.88069E-01
10	.1149E+06	.84273E-01
11	.1151E+06	.90508E-01
12	.1154E+06	.89430E-01
13	.1156E+06	.89047E-01
14	.1159E+06	.88795E-01
15	.1161E+06	.88583E-01
16	.1163E+06	.88467E-01
17	.1166E+06	.87907E-01
18	.1168E+06	.84594E-01
19	.1170E+06	.88798E-01
20	.1173E+06	.87833E-01
21	.1175E+06	.87859E-01
22	.1178E+06	.87360E-01
23	.1180E+06	.77738E-01
24	.1182E+06	.87806E-01
25	.1185E+06	.81945E-01
26	.1187E+06	.89330E-01
27	.1189E+06	.88522E-01
28	.1192E+06	.88067E-01
29	.1194E+06	.87903E-01
30	.1196E+06	.87721E-01
31	.1199E+06	.87399E-01
32	.1201E+06	.87707E-01
33	.1204E+06	.87497E-01
34	.1206E+06	.87370E-01
35	.1208E+06	.87260E-01
36	.1211E+06	.87157E-01
37	.1213E+06	.87058E-01
38	.1215E+06	.86960E-01
39	.1218E+06	.86844E-01
40	.1220E+06	.86846E-01
41	.1223E+06	.86723E-01
42	.1225E+06	.86630E-01
43	.1227E+06	.86542E-01
44	.1230E+06	.86455E-01
45	.1232E+06	.86368E-01
46	.1234E+06	.86276E-01
47	.1237E+06	.86163E-01
48	.1239E+06	.86517E-01
49	.1242E+06	.86112E-01
50	.1244E+06	.86012E-01

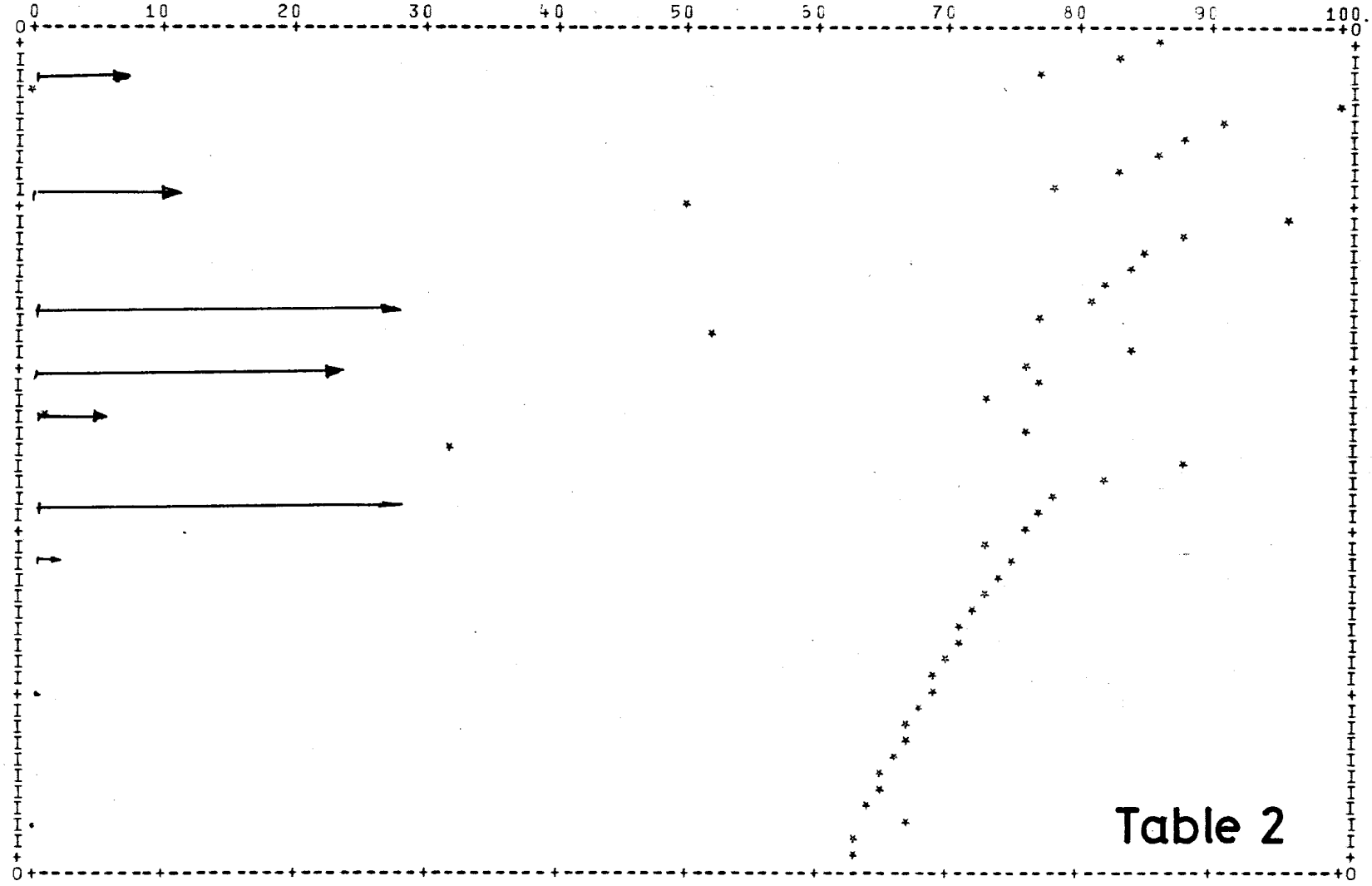

Table 2

ESTIMATE OF INTEGRAL... 1033.

TABLE AND PLOT OF THE FUNCTION AVSF

ABSCISSA PARAMETERS=
LOWER LIMIT... .21189E+06
UPPER LIMIT... .22928E+06
STEP SIZE..... 347.88
POINT NUMBER.. 51

ORDINATE PARAMETERS=
LOWER LIMIT... .54130E-01
UPPER LIMIT... .55536E-01
BIN SIZE..... .14056E-04
BIN NUMBER.... 100

POINT	ABSCISSA	ORDINATE
0	.21189E+06	.55536E-01
1	.21224E+06	.55106E-01
2	.21258E+06	.54898E-01
3	.21293E+06	.54775E-01
4	.21328E+06	.54691E-01
5	.21363E+06	.54630E-01
6	.21398E+06	.54583E-01
7	.21432E+06	.54545E-01
8	.21467E+06	.54513E-01
9	.21502E+06	.54486E-01
10	.21537E+06	.54462E-01
11	.21572E+06	.54441E-01
12	.21606E+06	.54422E-01
13	.21641E+06	.54404E-01
14	.21676E+06	.54388E-01
15	.21711E+06	.54373E-01
16	.21745E+06	.54359E-01
17	.21780E+06	.54345E-01
18	.21815E+06	.54333E-01
19	.21850E+06	.54320E-01
20	.21885E+06	.54309E-01
21	.21919E+06	.54298E-01
22	.21954E+06	.54287E-01
23	.21989E+06	.54276E-01
24	.22024E+06	.54266E-01
25	.22059E+06	.54256E-01
26	.22093E+06	.54247E-01
27	.22128E+06	.54238E-01
28	.22163E+06	.54229E-01
29	.22198E+06	.54220E-01
30	.22233E+06	.54211E-01
31	.22267E+06	.54203E-01
32	.22302E+06	.54195E-01
33	.22337E+06	.54187E-01
34	.22372E+06	.54180E-01
35	.22406E+06	.54173E-01
36	.22441E+06	.54166E-01
37	.22476E+06	.54159E-01
38	.22511E+06	.54153E-01
39	.22546E+06	.54148E-01
40	.22580E+06	.54142E-01
41	.22615E+06	.54138E-01
42	.22650E+06	.54134E-01
43	.22685E+06	.54132E-01
44	.22720E+06	.54130E-01
45	.22754E+06	.54131E-01
46	.22789E+06	.54134E-01
47	.22824E+06	.54141E-01
48	.22859E+06	.54153E-01
49	.22893E+06	.54176E-01
50	.22928E+06	.54217E-01

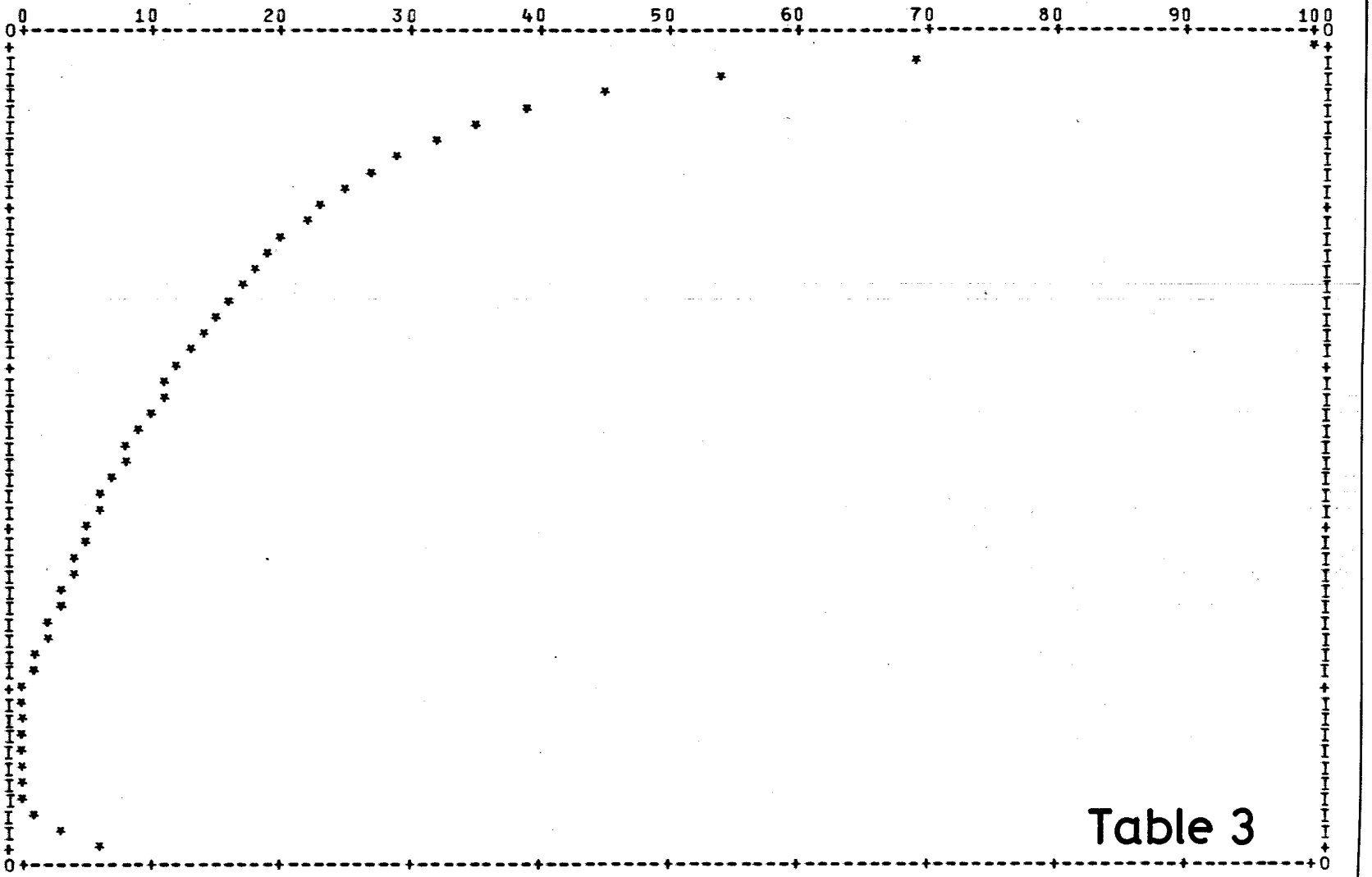

Table 3

ESTIMATE OF INTEGRAL... 945.1

TABLE AND PLOT OF THE FUNCTION AVSNZ

ABSCISSA PARAMETERS=
LOWER LIMIT... 17110.
UPPER LIMIT... 57034.
STEP SIZE..... 814.78
POINT NUMBER.. 50

ORDINATE PARAMETERS=
LOWER LIMIT... .34737E-01
UPPER LIMIT... .74023E-01
BIN SIZE..... .39285E-03
BIN NUMBER.... 100

POINT	ABSCISSA	L(m)	ORDINATE
0	17110.	10.45	.74023E-01
1	17925.		.71613E-01
2	18740.	9.53	.69412E-01
3	19555.		.67391E-01
4	20369.	9.58	.65529E-01
5	21184.		.63806E-01
6	21999.	9.22	.62206E-01
7	22814.		.60716E-01
8	23629.	8.89	.59324E-01
9	24443.		.58019E-01
10	25258.	8.60	.56794E-01
11	26073.		.55640E-01
12	26888.	8.34	.54552E-01
13	27702.		.53523E-01
14	28517.	8.10	.52548E-01
15	29332.		.51623E-01
16	30147.	7.87	.50744E-01
17	30962.		.49907E-01
18	31776.	7.67	.49108E-01
19	32591.		.48346E-01
20	33406.	7.48	.47617E-01
21	34221.		.46920E-01
22	35035.	7.30	.46251E-01
23	35850.		.45609E-01
24	36665.	7.14	.44993E-01
25	37480.		.44401E-01
26	38295.	6.99	.43830E-01
27	39109.		.43281E-01
28	39924.	6.84	.42751E-01
29	40739.		.42240E-01
30	41554.	6.71	.41747E-01
31	42368.		.41270E-01
32	43183.	6.58	.40808E-01
33	43998.		.40362E-01
34	44813.	6.46	.39929E-01
35	45628.		.39510E-01
36	46442.	6.34	.39103E-01
37	47257.		.38709E-01
38	48072.	6.23	.38326E-01
39	48887.		.37954E-01
40	49701.	6.13	.37592E-01
41	50516.		.37240E-01
42	51331.	6.03	.36898E-01
43	52146.		.36565E-01
44	52961.	5.94	.36241E-01
45	53775.		.35925E-01
46	54590.	5.85	.35617E-01
47	55405.		.35316E-01
48	56220.	5.77	.35023E-01
49	57034.		.34737E-01

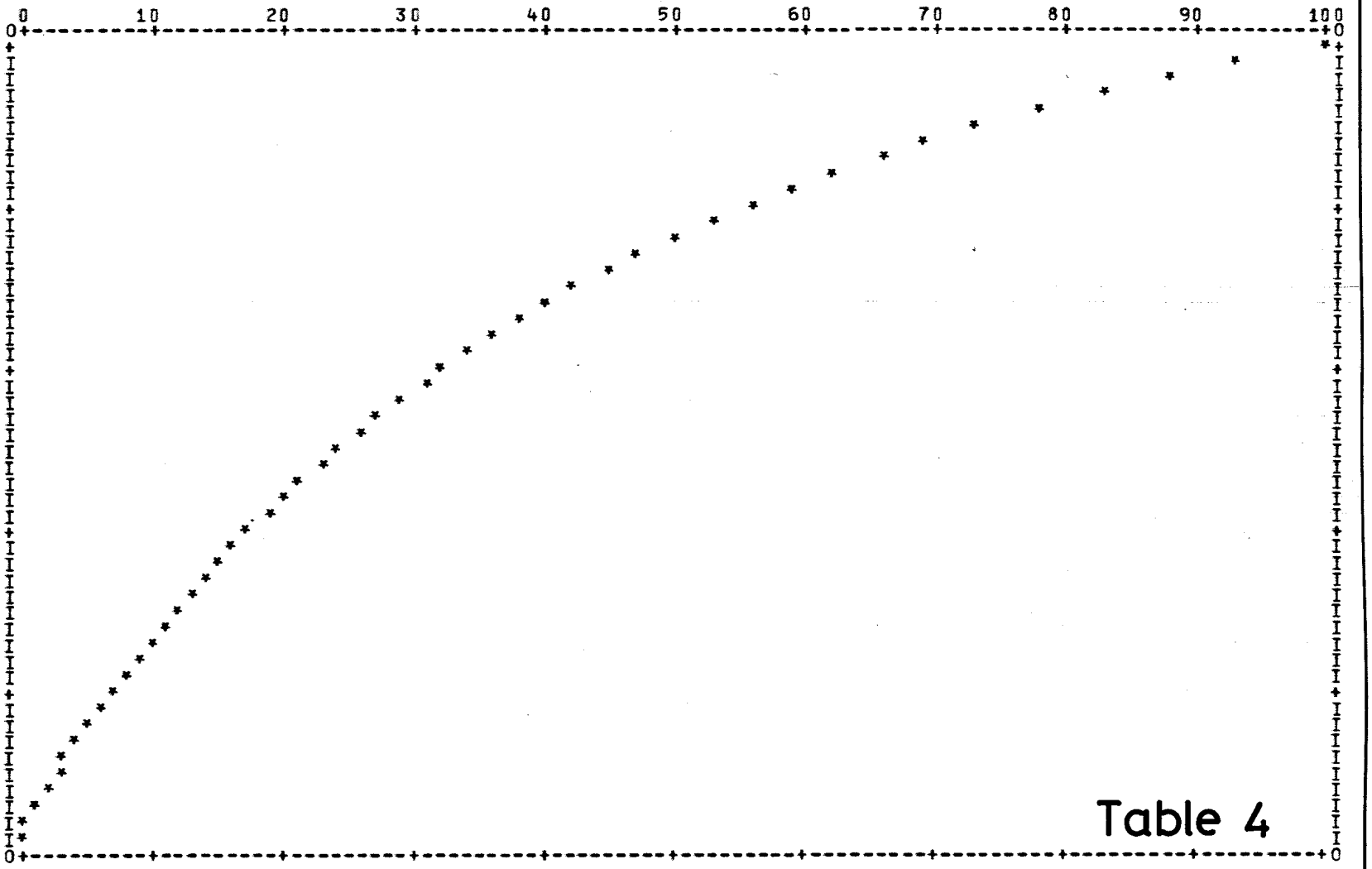

Table 4

ESTIMATE OF INTEGRAL... 1896.

ABSCISSA PARAMETERS=
LOWER LIMIT... .21189E+06
UPPER LIMIT... .22928E+06
STEP SIZE..... 347.88
POINT NUMBER.. 51

ORDINATE PARAMETERS=
LOWER LIMIT... 5273.0
UPPER LIMIT... .31432E+06
BIN SIZE..... 3090.5
BIN NUMBER.... 100

POINT	L(m)	ABSCISSA	ORDINATE
0	18.83	.21189E+06	5273.0
1	15.11	.21224E+06	7512.2
2	14.14	.21258E+06	9343.6
3	13.09	.21293E+06	10898.
4	12.35	.21328E+06	12257.
5		.21363E+06	13476.
6	11.32	.21398E+06	14592.
7		.21432E+06	15633.
8	10.60	.21467E+06	16620.
9		.21502E+06	17568.
10	10.05	.21537E+06	18489.
11		.21572E+06	19394.
12	9.60	.21606E+06	20291.
13		.21641E+06	21188.
14	9.20	.21676E+06	22092.
15		.21711E+06	23008.
16	8.83	.21745E+06	23941.
17		.21780E+06	24899.
18	8.50	.21815E+06	25885.
19		.21850E+06	26906.
20	8.17	.21885E+06	27967.
21		.21919E+06	29074.
22	7.86	.21954E+06	30235.
23		.21989E+06	31455.
24	7.55	.22024E+06	32743.
25		.22059E+06	34107.
26	7.25	.22093E+06	35558.
27		.22128E+06	37106.
28	6.94	.22163E+06	38763.
29		.22198E+06	40546.
30	6.63	.22233E+06	42470.
31		.22267E+06	44556.
32	6.32	.22302E+06	46826.
33		.22337E+06	49311.
34	5.96	.22372E+06	52042.
35		.22406E+06	55062.
36	5.66	.22441E+06	58422.
37		.22476E+06	62183.
38	5.36	.22511E+06	66427.
39		.22546E+06	71254.
40	4.93	.22580E+06	76796.
41		.22615E+06	83229.
42	4.54	.22650E+06	90789.
43		.22685E+06	99804.
44	4.11	.22720E+06	.11074E+06
45	3.88	.22754E+06	.12430E+06
46	3.63	.22789E+06	.14155E+06
47	3.31	.22824E+06	.16426E+06
48	3.09	.22859E+06	.19548E+06
49	2.78	.22893E+06	.24115E+06
50	2.44	.22928E+06	.31432E+06

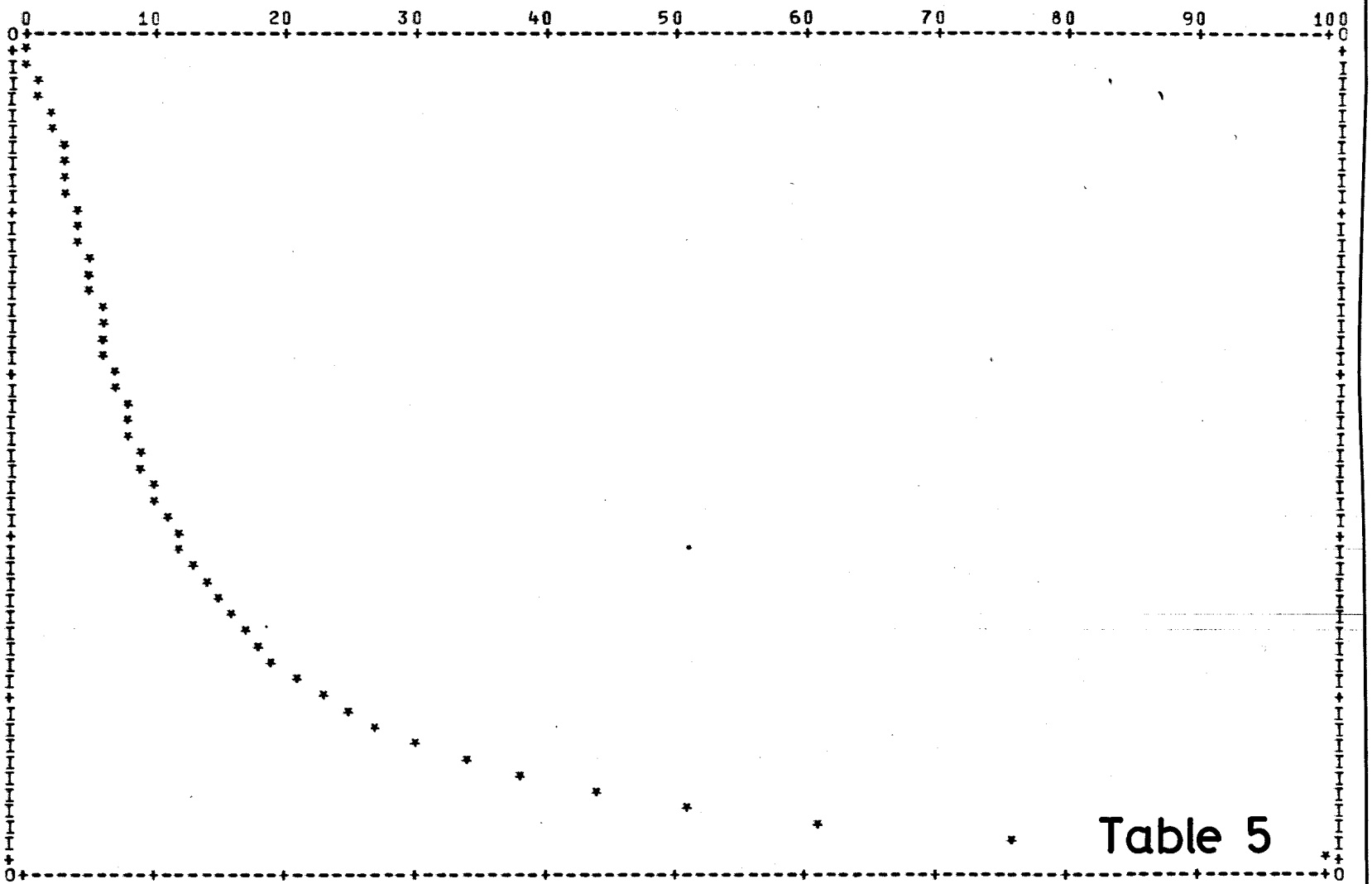

Table 5

ESTIMATE OF INTEGRAL... .9455E+09

TABLE AND PLOT OF THE FUNCTION AVSBMA

ABSCISSA PARAMETERS=
LOWER LIMIT... 0.
UPPER LIMIT... .10000E-06
STEP SIZE..... .20000E-08
POINT NUMBER.. 51

ORDINATE PARAMETERS=
LOWER LIMIT... .97831E-01
UPPER LIMIT... .10086
BIN SIZE..... .30326E-04
BIN NUMBER.... 100

POINT	ABSCISSA	ORDINATE
0	0.	.10085
1	.2000E-08	.10081
2	.4000E-08	.10075
3	.6000E-08	.10069
4	.8000E-08	.10063
5	.1000E-07	.10057
6	.1200E-07	.10051
7	.1400E-07	.10045
8	.1600E-07	.10039
9	.1800E-07	.10034
10	.2000E-07	.10028
11	.2200E-07	.10022
12	.2400E-07	.10016
13	.2600E-07	.10010
14	.2800E-07	.10004
15	.3000E-07	.99979E-01
16	.3200E-07	.99920E-01
17	.3400E-07	.99860E-01
18	.3600E-07	.99800E-01
19	.3800E-07	.99740E-01
20	.4000E-07	.99680E-01
21	.4200E-07	.99619E-01
22	.4400E-07	.99559E-01
23	.4600E-07	.99498E-01
24	.4800E-07	.99438E-01
25	.5000E-07	.99377E-01
26	.5200E-07	.99317E-01
27	.5400E-07	.99255E-01
28	.5600E-07	.99195E-01
29	.5800E-07	.99134E-01
30	.6000E-07	.99073E-01
31	.6200E-07	.99012E-01
32	.6400E-07	.98950E-01
33	.6600E-07	.98889E-01
34	.6800E-07	.98827E-01
35	.7000E-07	.98766E-01
36	.7200E-07	.98704E-01
37	.7400E-07	.98642E-01
38	.7600E-07	.98581E-01
39	.7800E-07	.98519E-01
40	.8000E-07	.98457E-01
41	.8200E-07	.98395E-01
42	.8400E-07	.98332E-01
43	.8600E-07	.98270E-01
44	.8800E-07	.98208E-01
45	.9000E-07	.98145E-01
46	.9200E-07	.98083E-01
47	.9400E-07	.98020E-01
48	.9600E-07	.97957E-01
49	.9800E-07	.97894E-01
50	.1000E-06	.97831E-01

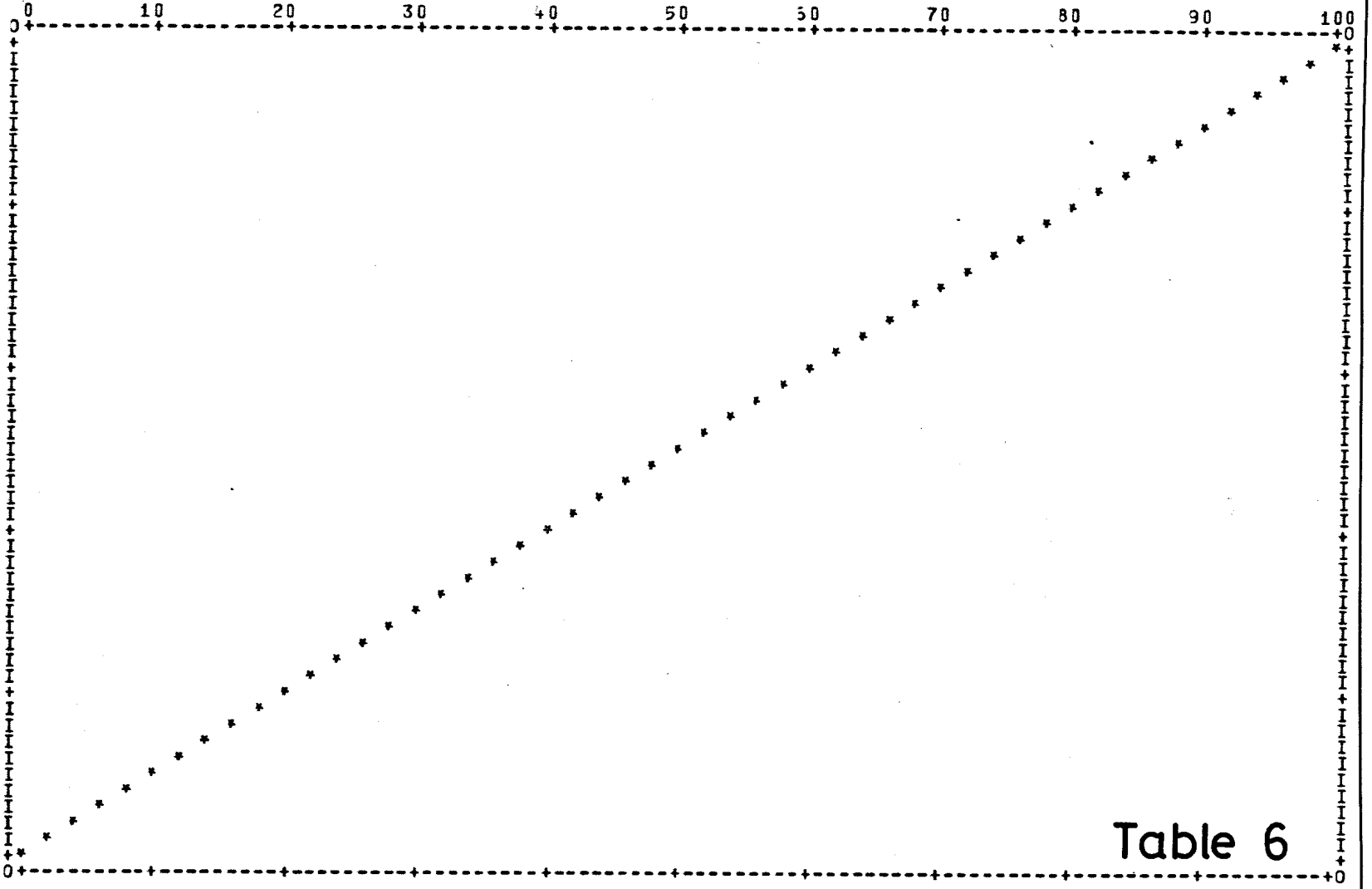

Table 6

ESTIMATE OF INTEGRAL... .9937E-08

TABLE AND PLOT OF THE FUNCTION AVSBMA

ABSCISSA PARAMETERS=		ORDINATE PARAMETERS=	
LOWER LIMIT...	0.	LOWER LIMIT...	.48702E-01
UPPER LIMIT...	.40000E-01	UPPER LIMIT...	.10086
STEP SIZE.....	.16000E-02	BIN SIZE.....	.52162E-03
POINT NUMBER..	26	BIN NUMBER....	100

POINT	ABSCISSA	ORDINATE
0	0.	.10086
1	.16000E-02	.48702E-01
2	.32000E-02	.49263E-01
3	.48000E-02	.49788E-01
4	.64000E-02	.50278E-01
5	.80000E-02	.50735E-01
6	.96000E-02	.51163E-01
7	.11200E-01	.51565E-01
8	.12800E-01	.51942E-01
9	.14400E-01	.52298E-01
10	.16000E-01	.52634E-01
11	.17600E-01	.52951E-01
12	.19200E-01	.53251E-01
13	.20800E-01	.53537E-01
14	.22400E-01	.53807E-01
15	.24000E-01	.54065E-01
16	.25600E-01	.54310E-01
17	.27200E-01	.54543E-01
18	.28800E-01	.54766E-01
19	.30400E-01	.54978E-01
20	.32000E-01	.55182E-01
21	.33600E-01	.55376E-01
22	.35200E-01	.55562E-01
23	.36800E-01	.55741E-01
24	.38400E-01	.55912E-01
25	.40000E-01	.56076E-01

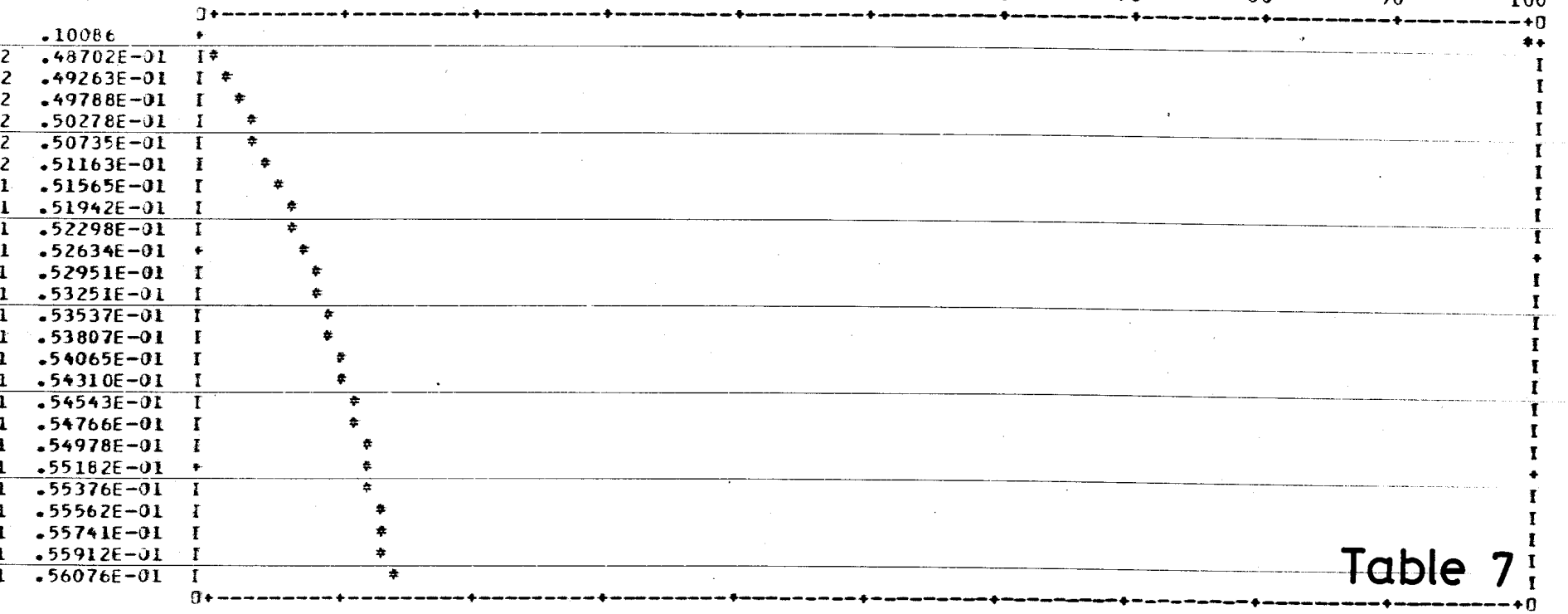

ESTIMATE OF INTEGRAL... .2161E-02

Table 7